APPLICATION OF SENTINEL-2 DATA TO ASSESS SEASONAL VEGETATION DYNAMICS IN THE IALPUG RIVER BASIN, SOUTHERN PART OF THE REPUBLIC OF MOLDOVA

Ecaterina MELNICENCO [1*], Viorica ANGHELUȚA [1], Iradion JECHIU [1] & Iurie BEJAN [1]

DOI: 10.21163/GT_2027.221.06

ABSTRACT

This study uses Sentinel-2 imagery to characterize seasonal vegetation dynamics in the analysed part of the Ialpug River Basin from March to October 2025. Monthly NDVI, month-to-month NDVI differences (ΔNDVI) and mean NDVI were calculated to describe vegetation greenness, the direction and magnitude of change between observations, and average greenness across the study period. The results show spring greening followed by spatially contrasting changes in early summer. Moderate vegetation cover occupied its largest share in April, while dense vegetation reached its maximum extent in June. The most widespread decline occurred between June and July, when 54.18% of the study area recorded an NDVI decrease exceeding 0.1. Very sparse vegetation reached its greatest extent in September, followed by limited greening in October. The mean NDVI classification placed 69.20% of the study area in the sparse vegetation class and 24.49% in the very sparse vegetation class, indicating predominantly low to intermediate average greenness across the selected observations. These classes do not establish persistent vegetation conditions or directly identify land-cover types. The summer decline coincided with documented regional drought conditions, but the analysis did not separate climatic effects from crop development, harvesting or other seasonal processes. The combined indicators provide complementary information for identifying areas with pronounced seasonal decline or low average greenness. Multi-year observations and independent climatic, land-cover and field evidence are required to determine the causes of these patterns and assess their longer-term environmental significance.

Keywords: *NDVI; Sentinel-2; Vegetation dynamics; Ialpug River Basin; Republic of Moldova.*

1. INTRODUCTION

Land degradation and aridization are key challenges in drought-prone regions where climatic stress, intensive land use and limited water availability interact. In the southern part of the Republic of Moldova, recurrent droughts, rising temperatures, reduced precipitation and the dominance of agricultural land make vegetation monitoring important for identifying areas exposed to environmental stress, desertification risk and the need for improved land and water management.

Remote sensing allows vegetation conditions to be monitored over large areas and through time. NDVI, based on red and near-infrared reflectance, is widely used to assess green biomass, vegetation activity and seasonal change. Although it does not directly measure land degradation, it can indicate vegetation stress and help identify areas affected by drought or other pressures. Recent European studies demonstrate that Sentinel-2 time series are particularly effective for analysing seasonal vegetation dynamics and land surface phenology. Study (Meroni et al., 2021) showed that Sentinel-2

[1] *State University of Moldova, Institute of Ecology and Geography, Chisinau, MD-2009, The Republic of Moldova. Corresponding author*: melnicenco.ecaterina@usm.md (ME); viorica.angheluta@sti.usm.md (VA); iradion.jechiu@sti.usm.md (IJ); iurie.bejan@sti.usm.md (IB).*

NDVI trajectories can distinguish the phenological development of major European crops, including wheat, barley, maize and sunflower, highlighting the strong influence of crop cycles on seasonal vegetation index patterns. Furthermore (Tian et al., 2021) further demonstrated that Sentinel-2 vegetation indices can reliably characterize the timing of seasonal vegetation development across different European ecosystems.

The Ialpug River Basin was selected because it lies in the southern part of the Republic of Moldova, one of the country's areas most exposed to drought and aridization (Guvernul Republicii Moldova, 2024). This vulnerability is linked to declining warm-season precipitation, rising temperatures, higher evaporative demand and reduced surface-water availability. Average annual precipitation decreased by about 14 mm, or 3%, between 1961–1990 and 1991–2020, while southern and south-eastern parts of Republic of Moldova remained among the driest areas of the country (Serviciul Hidrometeorologic de Stat, 2022). Drought severity has also increased, with 2011–2020 identified as Moldova's warmest decade and post-2000 droughts amplified by higher atmospheric evaporative demand (Vicente-Serrano et al., 2024). Runoff volumes declined during 1977–2022, 2011–2022 were classified as dry years, and water use increased during drought years such as 2007, 2009, 2020 and 2022 (Burduja and Bacal, 2023). The southern part of the Republic of Moldova is also identified as the most vulnerable agro-climatic region, with a dry hydrothermal regime and increasing moisture deficit. In the Ialpug River Basin, flow reconstruction near Comrat shows that mean river flow decreased by approximately half between 1962–1989 and 1990–2016, with the strongest seasonal reduction in spring, followed by summer and winter (Jeleapov, 2024). Agricultural land use, fragmented vegetation cover and limited water resources make the basin suitable for analysing seasonal vegetation dynamics through satellite-based methods (Phiri et al., 2020).

This study aims to determine whether the combined analysis of monthly NDVI, ΔNDVI and growing-season mean NDVI can identify the timing, magnitude and spatial distribution of vegetation decline in the Ialpug River Basin during the March–October 2025 vegetation period. Its contribution goes beyond standard GIS-based NDVI calculation by integrating three complementary temporal indicators: monthly NDVI for vegetation condition at individual growing-season stages, ΔNDVI for the direction and magnitude of month-to-month change, and mean NDVI for average vegetation greenness across the analysed period. Interpreted together, these indicators provide a basin-scale assessment of intra-seasonal vegetation dynamics and reduce the risk of treating a single low-NDVI observation as evidence of land degradation.

2. STUDY AREA

The Ialpug River Basin is located in the southern part of the Republic of Moldova and extends into Ukraine (**Fig. 1**). It lies within the Bugeac Steppe and has an elongated north–south shape, with a wider central section. This area is among the driest and the most vulnerable to climatic vulnerability regions of the Republic of Moldova.

The Ialpug River flows predominantly from north to south through the southern part of the Republic of Moldova, almost parallel to the Prut River. After leaving the territory of the Republic of Moldova, it enters Ukraine and discharges into Lake Ialpug. Its main tributaries include Ialpugeni, Salcia Mare, Lunga, Lunguța and Sar-Iar. The basin covers a total area of 3,180 km² and includes parts of Cahul, Basarabeasca, Cantemir, Cimișlia, Hâncești, Leova and Taraclia districts, as well as the Autonomous Territorial Unit of Gagauzia (Chiriac and Sirodoev, 2025). It also includes important urban centres such as Comrat, Ceadâr-Lunga and Taraclia, which makes the basin relevant not only from a physical-geographic perspective, but also for land use, water management and socioeconomic analysis. The study area comprises the part of the basin located within the Republic of Moldova representing 71.35% of the basin's total area, as shown in **Fig. 1**.

The Ialpug River Basin boundary was delineated in QGIS using a 35 m spatial resolution Shuttle Radar Topography Mission (SRTM) digital elevation model (DEM). Basin extraction was performed with the *r.watershed* algorithm available through the GRASS GIS processing tools in QGIS. The relevant hydrological parameters were adjusted to obtain the drainage area corresponding to the Ialpug

River Basin. The resulting raster watershed boundary was subsequently converted into a vector polygon in shapefile format and used as the spatial boundary for clipping and analysing the Sentinel-2-derived NDVI datasets.

To define the spatial extent used for the analysis, the derived Ialpug Basin polygon was overlaid with the national boundary of the Republic of Moldova. This spatial operation resulted in four polygon fragments, from which two located within the Republic of Moldova and two within Ukraine. One small, spatially disconnected polygon, representing approximately 1% of the delineated area, was excluded from further calculations because it formed an isolated fragment rather than part of the main contiguous study area. Consequently, the subsequent Sentinel-2 and NDVI analyses were performed for the main contiguous polygon representing the principal part of the basin considered in the study. The final basin boundary was used for clipping the Sentinel-2 imagery and for all subsequent raster-based calculations and area statistics.

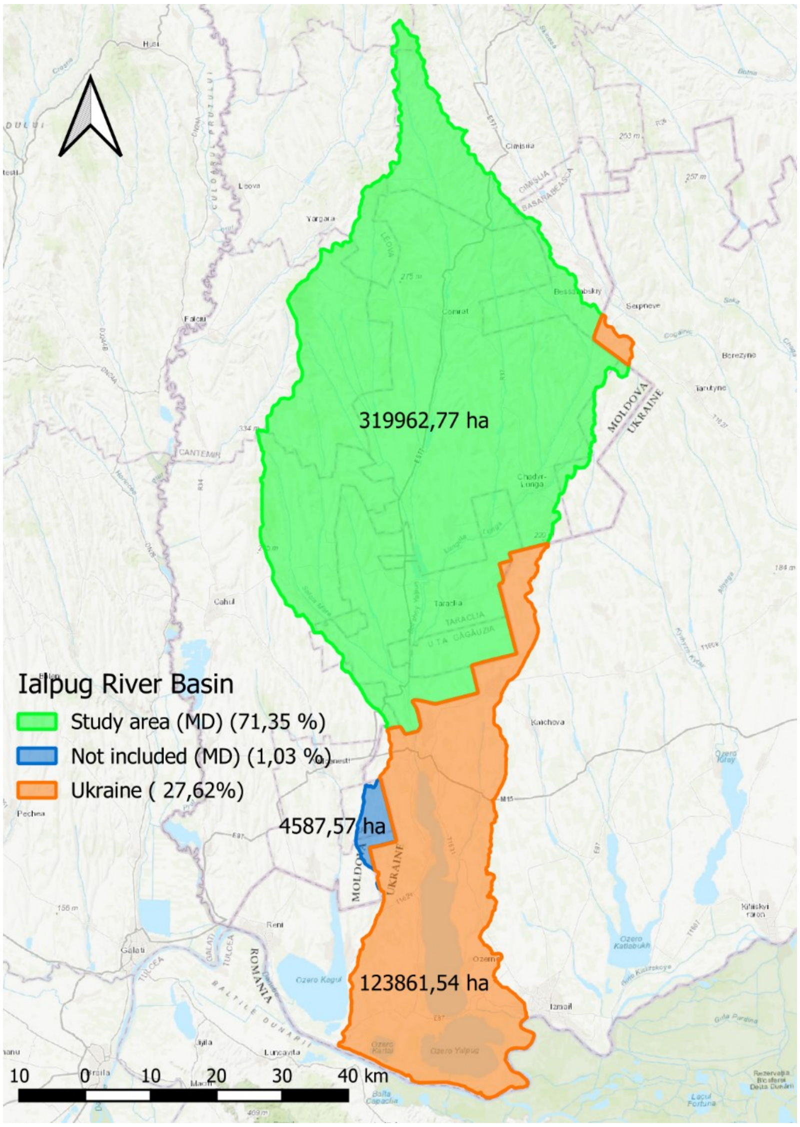

Fig. 1. The Ialpug River Basin.

3. DATA AND METHODS

3.1. NDVI as an indicator measuring vegetation dynamics

In recent decades satellite imagery has become an important source of spatially consistent information for landscape analysis. Its repeated coverage allows changes in land-surface characteristics to be examined across large areas and at successive observation dates.

In the current study, NDVI is used as an indicator of vegetation activity and its seasonal variation. Higher or lower NDVI values are interpreted in terms of relative vegetation activity, while their environmental causes cannot be determined from NDVI alone. Monthly satellite series for 2025 were used to identify the seasonal trends to examine the temporal and spatial variations in the vegetation greenness and activity. In the current study NDVI applies as integrative indicator of ecosystem conditions, because it reflects vegetation health and is widely applied in drought assessment due to the close relationship between precipitation, soil moisture and vegetation response (Serban and Maftei, 2025).

This approach is supported by recent European and Mediterranean studies demonstrating the use of NDVI for long-term vegetation monitoring, drought-resilience assessment, soil degradation and erosion detection, and landscape-fragmentation analysis. For example, long-term NDVI time series can be used to assess seasonal vegetation trends across Europe (Eisfelder et al., 2023). Satellite time series can support the assessment of vegetation resilience to drought under grazing pressure (von Keyserlingk et al., 2021). NDVI-based vegetation estimates may be less reliable in areas with low biomass density, a limitation considered when interpreting the present result (Smith and Boers, 2023). Varghese et al. (2021) demonstrated that Sentinel-2 data are suitable for drought assessment, particularly through vegetation indices such as NDVI, as well as indicators related to soil moisture, evapotranspiration, surface water and land-use and land-cover changes.

NDVI is based on the fact that the spectral reflectance from healthy vegetation differs from that of soil, sparse vegetation and water. Plant cells with chlorophyll absorb visible red radiation, while the internal structure of leaves strongly reflects near-infrared radiation. Tucker (1979) stated that combinations of red and photographic infrared bands are effective for monitoring vegetation conditions, as they are sensitive to green biomass, chlorophyll absorption and vegetation cover. This provides the methodological basis for using NDVI as an indicator of vegetation activity and seasonal vegetation dynamics. Consequently, areas with dense green vegetation have higher NDVI values, while bare soil, degraded surfaces, sparse vegetation or water bodies show lower values. NDVI was calculated as follows.

$$NDVI = \frac{B8-B4}{B8+B4} \tag{1}$$

where:

NDVI	Normalized Difference Vegetation Index
B8	Near-Infrared Spectral Band
B4	Red Spectral Band

Despite having been used for several decades, NDVI remains one of the most widely applied remote-sensing indices for vegetation assessment because it is accessible, computationally simple and supported by numerous satellite sensors (Huang et al., 2021; Karlsen et al., 2021; Rossi, Krtalić and Buzjak, 2025). NDVI values range from -1 to +1, with negative values generally linked to water or non-vegetated surfaces, values close to zero linked to bare soil or sparse vegetation, and higher positive values indicating progressively greater vegetation greenness.

3.2. Calculation of NDVI from Sentinel-2 imagery

Sentinel-2 imagery is widely used for land-cover and vegetation monitoring because of their high spatial resolution, frequent revisit interval, open availability and suitability for mapping crops, forests, urban areas and water bodies. (Phiri et al., 2020). NDVI has also been applied to monitor different vegetation types, including forests (Govedar and Anikić, 2024).

The analysis used Sentinel-2 Level-2A surface-reflectance imagery obtained from the Copernicus Data Space Ecosystem for eight observation periods between March and October 2025. Two Sentinel-2 tiles were required to cover the analysed part of the Ialpug River Basin: tile 35TPL for the southern sector and tile 35TPM for the northern sector. NDVI was calculated from Band 4 (B04 – red, 665 nm) and Band 8 (B08 – near-infrared, 842 nm), both of which have a spatial resolution of 10 m. The imagery was processed in the WGS 84 / UTM zone 35N coordinate reference system. **Table 1** presents the product identifiers, sensing dates, scene-level cloud cover and other acquisition metadata.

Table 1.

Sentinel-2 images used for the study.

Month	Name	Size	Sensing time	Cloud cover, %	Tile identifiers
March	S2C_MSIL2A_20250322T085651_N0511_R007_T35TPL_20250322T145857.SAFE	1,050 MB	2025-03-22T08:56:51.024000Z	0.072601	35TPL
	S2C_MSIL2A_20250322T085651_N0511_R007_T35TPM_20250322T145857.SAFE	1,078 MB	2025-03-22T08:56:51.024000Z	0.085358	35TPM
April	S2A_MSIL2A_20250423T085721_N0511_R007_T35TPL_20250423T173200.SAFE	1,049 MB	2025-04-23T08:57:21.024000Z	0.187979	35TPL
	S2C_MSIL2A_20250421T085621_N0511_R007_T35TPM_20250421T144609.SAFE	1,086 MB	2025-04-21T08:56:21.025000Z	0.63088	35TPM
May	S2C_MSIL2A_20250521T085611_N0511_R007_T35TPL_20250521T120515.SAFE	1,081 MB	2025-05-21T08:56:11.025000Z	3.278569	35TPL
	S2C_MSIL2A_20250521T085611_N0511_R007_T35TPM_20250521T120515.SAFE	1,097 MB	2025-05-21T08:56:11.025000Z	4.230152	35TPM
June	S2B_MSIL2A_20250618T090559_N0511_R050_T35TPL_20250618T113950.SAFE	453 MB	2025-06-18T09:05:59.024000Z	1.400214	35TPL
	S2C_MSIL2A_20250620T085611_N0511_R007_T35TPM_20250620T114819.SAFE	1,102 MB	2025-06-20T08:56:11.025000Z	0.278184	35TPM
July	S2B_MSIL2A_20250725T085559_N0511_R007_T35TPL_20250725T113316.SAFE	1,086 MB	2025-07-25T08:55:59.024000Z	0.063938	35TPL
	S2B_MSIL2A_20250725T085559_N0511_R007_T35TPM_20250725T113316.SAFE	1,119 MB	2025-07-25T08:55:59.024000Z	2.140666	35TPM
August	S2B_MSIL2A_20250827T090559_N0511_R050_T35TPL_20250827T101153.SAFE	440 MB	2025-08-27T09:05:59.024000Z	1.98649	35TPL
	S2B_MSIL2A_20250827T090559_N0511_R050_T35TPM_20250827T101153.SAFE	738 MB	2025-08-27T09:05:59.024000Z	0.000048	35TPM
September	S2C_MSIL2A_20250921T090711_N0511_R050_T35TPL_20250921T130414.SAFE	432 MB	2025-09-21T09:07:11.025000Z	0.015964	35TPL
	S2C_MSIL2A_20250921T090711_N0511_R050_T35TPM_20250921T130414.SAFE	730 MB	2025-09-21T09:07:11.025000Z	0.000302	35TPM
October	S2A_MSIL2A_20251020T090031_N0511_R007_T35TPL_20251020T125922.SAFE	1,078 MB	2025-10-20T09:00:31.024000Z	0.01706	35TPL
	S2A_MSIL2A_20251020T090031_N0511_R007_T35TPM_20251020T125922.SAFE	1,104 MB	2025-10-20T09:00:31.024000Z	2.528081	35TPM

For each month, one acquisition was selected for each of the two tiles. The northern and southern tiles were acquired on the same date in March, May, July, August, September and October. In April and June, the acquisition dates differed by two days. Consequently, the April and June mosaics should be understood as near-contemporaneous representations of the study area rather than strictly simultaneous observations.

Only Sentinel-2 scenes with less than 5% scene-level cloud cover were selected. Although limited cloud cover was present in some original scenes, inspection of the imagery confirmed that clouds and cloud shadows did not affect the study-area polygon. Therefore, no additional cloud or cloud-shadow masking was applied within the study area. No NoData pixels were identified within the analysed polygon. Pixels with negative NDVI values corresponded to water surfaces and were retained as a separate class. Accordingly, all pixels within the study-area polygon were included in the monthly NDVI, ΔNDVI and mean NDVI calculations.

For each observation period, the corresponding 35TPL and 35TPM tiles were mosaicked separately for B04 and B08 using the QGIS Merge algorithm. This procedure produced two raster layers for each month – Month_B04.tif and Month_B08.tif – covering the full study area. The merged spectral bands were saved as GeoTIFF files. The source-band data type was preserved during mosaicking, while the subsequently calculated NDVI rasters retained continuous floating-point values.

A monthly NDVI raster was calculated from each pair of mosaicked B04 and B08 bands using the QGIS Raster Calculator and the standard NDVI formula presented in Equation 1. In QGIS syntax, the calculation was expressed as:

("B8@1" − "B4@1")/("B8@1" + "B4@1") (2)

The monthly NDVI rasters were reclassified into the five descriptive classes presented in **Table 2** using the QGIS Reclassify by Table algorithm. The interval rule minimum less than or equal to value and value less than maximum was applied to the first four classes, while the final class included the upper NDVI limit of 1. The reclassified rasters were stored as integer-class GeoTIFF files. The number of pixels assigned to each class within the study-area polygon was calculated and converted into a percentage of the total number of analysed pixels. All spatial processing was performed in QGIS version 3.40.4-Bratislava.

Table 2.

NDVI value intervals and their classification.

NDVI values	Interpretation
-1 to 0	Water bodies, clouds or other non-vegetated areas
0 to 0.2	Bare land, exposed soil, built-up areas, very sparse vegetation
0.2 to 0.4	Sparse vegetation, degraded steppe vegetation, stressed vegetation
0.4 to 0.6	Moderate vegetation cover, active vegetation phase
0.6 to 1.0	Dense and healthy vegetation cover

Zonal statistics were then applied using the Ialpug River Basin boundary in order to calculate the distribution and statistical characteristics of NDVI values within the study area.

3.3. Application of ΔNDVI to assess the vegetation dynamics

In addition to the analysis of absolute NDVI values, the study calculated the ΔNDVI to evaluate changes in vegetation condition between different periods of the growing season. While NDVI shows the state of vegetation at a specific moment, ΔNDVI allows the identification of spatial and temporal changes by comparing NDVI values from two successive observation dates. NDVI differencing has been used to investigate longer-term vegetation decline and support landscape planning in Mediterranean regions (Gabriele et al., 2023).

ΔNDVI represents the change in NDVI values between two consecutive months and was calculated as the difference between the later NDVI value and the earlier NDVI value. In this study, ΔNDVI was used to assess seasonal vegetation dynamics in the Ialpug River Basin and to identify areas where vegetation cover increased, decreased or remained relatively stable.

Positive ΔNDVI values indicate an increase in vegetation activity, usually associated with vegetation growth, regeneration or improved moisture conditions. Negative ΔNDVI values indicate a decrease in vegetation activity, which may reflect drought stress, drying of vegetation, harvesting, or other land use changes. Values close to zero indicate limited change in NDVI between the two observation dates.

For the analysis, ΔNDVI values were grouped into three classes: decrease for values below −0.1, minor change for values from −0.1 to 0.1, and increase for values above 0.1. These thresholds describe the numerical magnitude of change and do not indicate statistical significance. This approach made it possible to identify spatial patterns of vegetation decrease, minor change and increase between consecutive observations. Negative ΔNDVI may indicate vegetation senescence, harvesting, reduced moisture availability or other seasonal land-surface changes; therefore, it is not interpreted independently as evidence of vegetation degradation.

3.4. Calculation of growing season mean NDVI

To assess the general vegetation condition in the Ialpug River Basin, the study calculated the mean NDVI for the growing season from March to October. Monthly NDVI raster layers were first generated for each analysed month using Sentinel-2 data. These layers were then combined into a single raster representing the average NDVI value for each pixel over the selected period.

This approach made it possible to reduce the influence of short-term fluctuations and to identify the average vegetation greenness during the full growing season. Unlike monthly NDVI maps, which show vegetation status at a specific moment, the mean NDVI map provides an integrated picture of relative vegetation activity across the analysed growing season and reduces the influence of individual short-term observations.

Following its calculation, the mean NDVI raster was clipped to the Ialpug River Basin boundary and reclassified into vegetation-condition categories using threshold values consistent with the NDVI classification presented in **Table 2**.

3.5. National climatic context used for the interpretation

Regional agrometeorological information for summer 2025 was obtained from the State Hydrometeorological Service of the Republic of Moldova to support the interpretation of the observed vegetation dynamics (Serviciul Hidrometeorologic de Stat, 2025). The source describes temperature, precipitation, drought and soil-moisture conditions, including observations from meteorological stations in southern Moldova such as Comrat, Ceadâr-Lunga and Cahul.

The climatic information was used only as contextual evidence for interpreting the temporal correspondence between the observed NDVI patterns and regional agrometeorological conditions. Climatic variables were not spatially matched with Sentinel-2 pixels and no statistical relationships between NDVI, and temperature, precipitation, soil moisture or Standardized Precipitation Evapotranspiration Index (SPEI) were evaluated in the present study. Consequently, climatic conditions are used to identify temporal correspondence rather than to establish causality.

4. RESULTS

The results are presented through three complementary NDVI analyses: monthly NDVI, ΔNDVI and mean NDVI. Together, they show the seasonal development, month-to-month change and average vegetation greenness of the Ialpug River Basin during March–October 2025.

4.1. Monthly NDVI Dynamics

The monthly NDVI maps describe vegetation greenness in the analysed part of the Ialpug River Basin from March to October 2025. **Table 3** presents the monthly percentage distribution of the five NDVI classes defined in **Table 2**.

Table 3.

Monthly distribution of NDVI classes in the Ialpug River Basin, March–October 2025 (%).

Month	**Non vegetated areas (−1 to 0)**	**Very sparse vegetation (0 to 0.2)**	**Sparse vegetation (0.2 to 0.4)**	**Moderate vegetation cover (0.4 to 0.6)**	**Dense vegetation (0.6 to 1.0)**
March	0.48	41.60	42.66	15.08	0.18
April	0.42	28.66	26.90	39.86	4.16
May	0.43	27.79	29.73	38.59	3.46
June	0.33	22.99	40.56	30.92	5.20
July	0.25	52.16	37.20	10.33	0.06
August	0.29	67.71	25.68	6.28	0.04
September	0.21	73.52	21.48	4.78	0.01
October	0.28	66.78	28.29	4.63	0.02

In March, vegetation was still at an early development stage: sparse vegetation covered 42.66% of the basin, followed by very sparse vegetation at 41.60%. Moderate vegetation cover accounted for 15.08%, while dense vegetation represented 0.18% and non-vegetated areas accounted for 0.48%. This distribution indicates relatively limited vegetation activity at the beginning of the analysed growing season. In April, vegetation activity increased substantially. Moderate vegetation cover increased to 39.86%, becoming the dominant class, while very sparse vegetation declined to 28.66% and sparse vegetation to 26.90%. Dense vegetation increased to 4.16%, while non-vegetated areas accounted for 0.42%. In May, the distribution remained relatively similar, with moderate vegetation cover accounting for 38.59%, sparse vegetation for 29.73%, very sparse vegetation for 27.79%, dense vegetation for 3.46%, and non-vegetated areas for 0.43%. **Fig. 2** shows the distribution of NDVI values during the spring months.

In June, sparse vegetation became the dominant class, increasing to 40.56%, while moderate vegetation cover represented 30.92%. Very sparse vegetation declined further to 22.99% – its lowest share during the analysed period – while dense vegetation reached its seasonal maximum of 5.20%. Non-vegetated areas represented 0.33%. Thus, April–June was the period with the highest proportion of moderate and dense vegetation cover.

July marked a pronounced shift toward lower NDVI classes. Very sparse vegetation increased to 52.16%, while sparse vegetation accounted for 37.20%. Moderate vegetation cover declined sharply to 10.33%, and dense vegetation became almost absent at 0.06%. Non-vegetated areas represented 0.25%. July therefore was the month with the strongest observed reduction in vegetation activity during the analysed period. This pattern became even more pronounced in August and September. Very sparse vegetation increased to 67.71% in August and reached its seasonal maximum of 73.52% in September. At the same time, sparse vegetation declined from 25.68% in August to 21.48% in September, while moderate vegetation cover decreased from 6.28% to 4.78%.

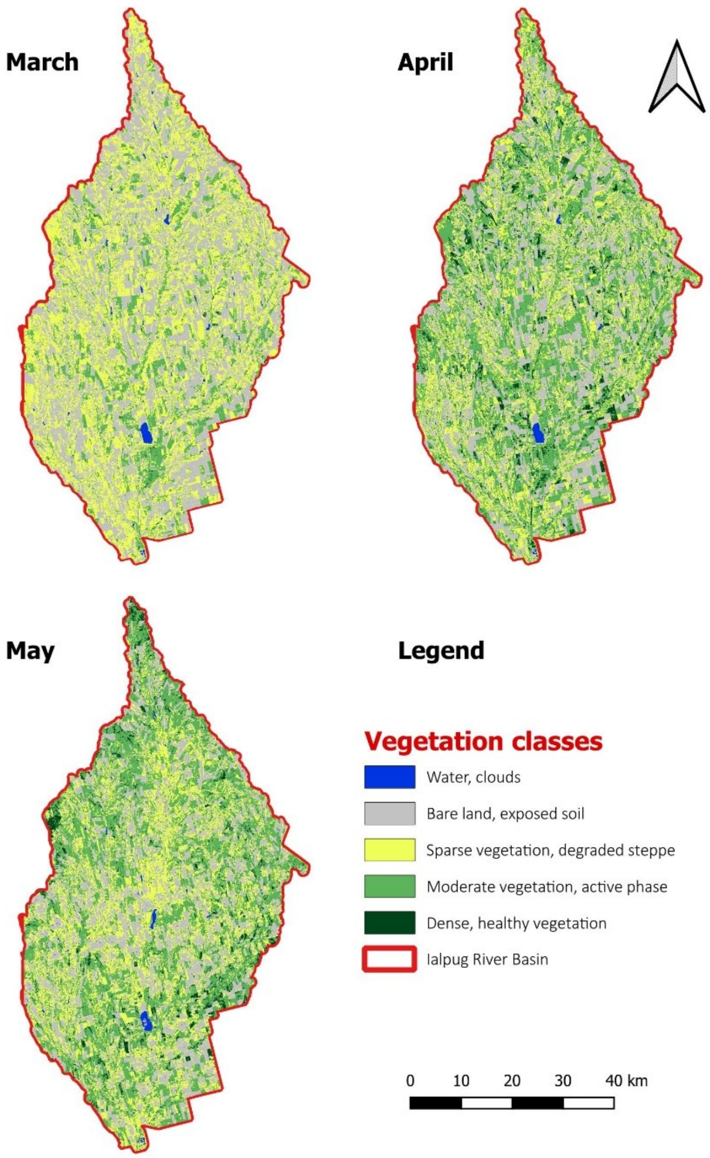

Fig. 2. Spatial distribution of NDVI values in the Ialpug River Basin during spring 2025.

Dense vegetation accounted for only 0.04% in August and 0.01% in September. Non-vegetated areas remained very limited, representing 0.29% and 0.21%, respectively.

In October, the distribution showed a limited shift compared with September. Very sparse vegetation decreased to 66.78%, while sparse vegetation increased to 28.29%. Moderate vegetation cover remained low at 4.63%, dense vegetation represented 0.02%, and non-vegetated areas accounted for 0.28%. The spatial distribution of NDVI values in the Ialpug River Basin during summer and autumn 2025 is presented in **Figs. 3 and 4**, respectively.

These results demonstrate strong seasonal variation in vegetation activity across the basin. From March to June, vegetation activity increased, reflected particularly in the expansion of moderate and dense vegetation classes.

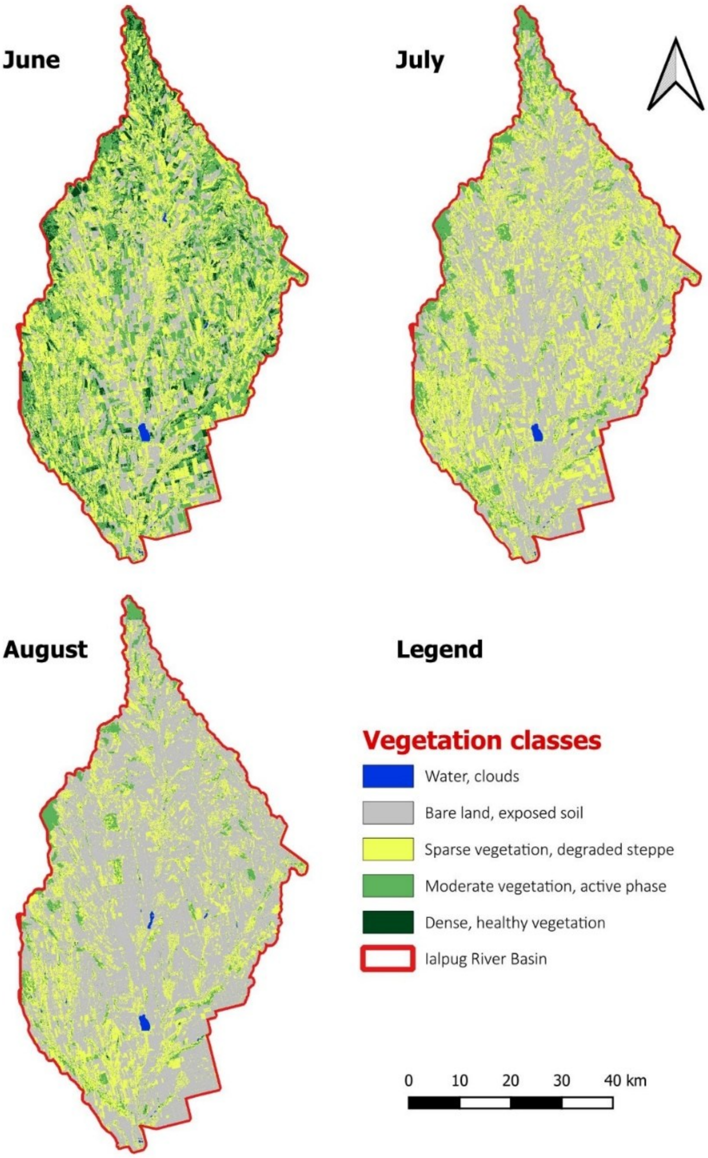

Fig. 3. Spatial distribution of NDVI values in the Ialpug River Basin during summer 2025.

From July to September, the distribution shifted strongly toward very sparse and sparse vegetation, accompanied by a substantial reduction in moderate and dense vegetation cover. In October, the overall low-NDVI pattern persisted, although the increase in sparse vegetation and decline in very sparse vegetation indicate a limited redistribution toward slightly higher NDVI values. Because the analysis covers only one growing season and does not independently separate land-cover classes or climatic effects, these patterns are interpreted as differences in seasonal vegetation persistence rather than evidence of ecological resilience or degradation. Monthly NDVI can support preliminary vegetation monitoring and help identify areas requiring further climatic, land-cover and field-based assessment.

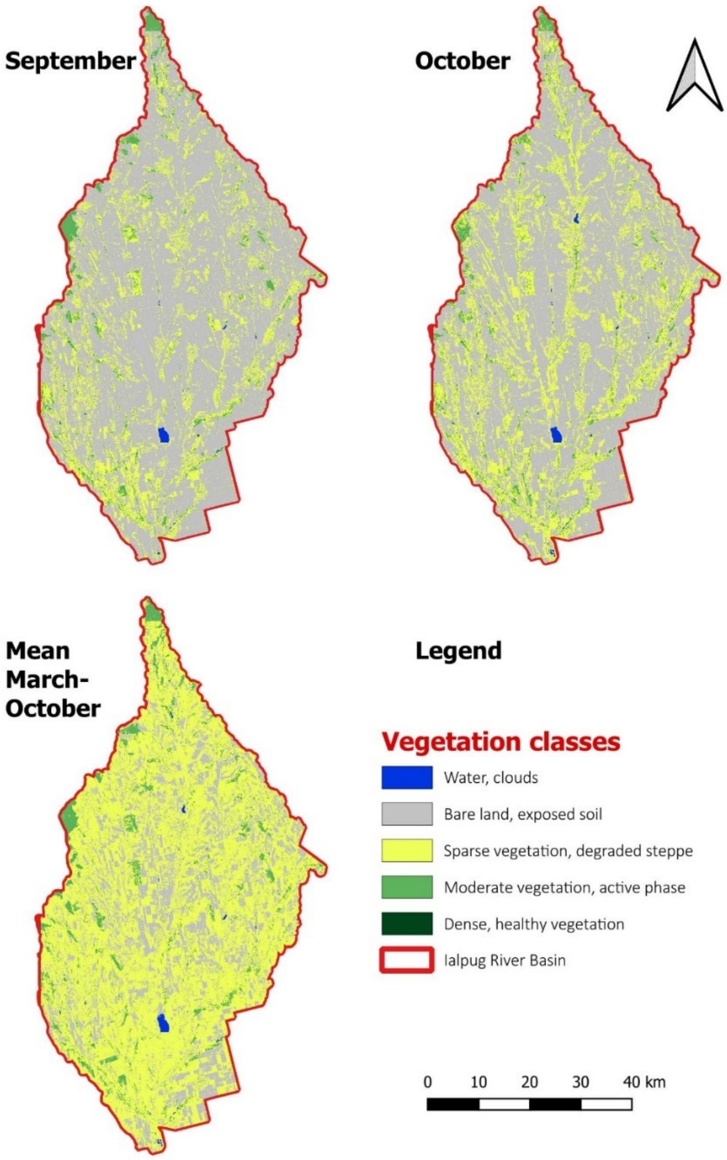

Fig. 4. Spatial distribution of NDVI values in the Ialpug River Basin during autumn 2025.

4.2. Application of ΔNDVI for assessing vegetation dynamics

The ΔNDVI analysis describes the direction and magnitude of change in vegetation between successive observation dates. Positive values indicate increasing NDVI, negative values indicate decreasing NDVI, and values close to zero indicate minor change. Based on the thresholds defined in the Methods, the results were divided into decrease, minor-change and increase classes. These classes represent numerical ranges and do not indicate statistical significance.

Between April and March, 45.24% of the study area recorded NDVI increases exceeding 0.1, while 54.17% fell within the minor-change class and 0.59% recorded decreases below −0.1. This distribution indicates widespread spring greening. This distribution can be explained by functional differentiation of the landscape: some crops and grasslands continue to develop, while others, especially early agricultural crops, begin to show the first reductions in photosynthetic activity, anticipating the summer decline.

Between May and April, minor change was the dominant class, accounting for 64.62% of the study area. NDVI increases exceeding 0.1 occurred across 18.11% of the area, while decreases below −0.1 accounted for 17.27%. The similar proportions of increase and decrease indicate spatially contrasting vegetation dynamics, although the underlying land-cover or crop-specific processes cannot be identified from NDVI alone.

The June to May interval showed the most balanced distribution among the three ΔNDVI classes. Decrease, minor change and increase accounted for 34.43%, 33.98% and 31.59% of the study area, respectively. This distribution may reflect several overlapping seasonal processes, including the maturation of winter crops, continued development of spring crops, stabilization of natural vegetation and the first effects of moisture deficit. However, the respective effects of crop phenology, harvesting, natural vegetation dynamics and moisture availability cannot be separated using the available data.

The largest spatial extent of decline occurred between July and June, when 54.18% of the study area recorded an NDVI decrease below −0.1. Minor change accounted for 44.28%, while increases exceeding 0.1 occurred across only 1.54% of the area. This widespread decline coincided with the transition towards predominantly low monthly NDVI values. It may be associated with several overlapping processes, including crop maturation, harvesting, vegetation senescence and the hot and dry regional conditions documented during summer 2025.

Between August and July, 84.22% of the study area fell within the minor-change class, while 14.82% recorded NDVI decreases below −0.1 and 0.96% recorded increases above 0.1. Monthly NDVI values nevertheless remained predominantly low. The dominance of minor changes therefore indicates limited change following the widespread June–July decline, rather than a general recovery of vegetation condition.

Between September and August, 97.79% of the study area showed minor change, while 1.89% recorded decreases and 0.32% recorded increases beyond the adopted thresholds. Between October and September, minor change remained dominant at 92.16%, while increases accounted for 6.42% and decreases for 1.42%. The latter interval indicates localized greening, although the monthly distribution remained dominated by low NDVI class. However, this recovery remained limited and did not compensate for summer vegetation decline. The percentage distribution of the three ΔNDVI classes for each analysed period is presented in **Table 4**.

Table 4.

Percentage distribution of ΔNDVI classes in the analysed part of the Ialpug River Basin during the 2025 growing season (%).

Observation interval	Decrease (<-0.1) %	Minor change (-−0.1 to 0.1) %	Increase (>0.1) %
April - March	0.59	54.17	45.24
May - April	17.27	64.62	18.11
June - May	34.43	33.98	31.59
July - June	54.18	44.28	1.54
August - July	14.82	84.22	0.96
September - August	1.89	97.79	0.32
October - September	1.42	92.16	6.42

Overall, the ΔNDVI results show spatially differentiated seasonal dynamics, including widespread spring greening, contrasting changes between May and June, the largest extent of decline between June and July, and limited localized greening between September and October. ΔNDVI complements the monthly maps by identifying when and where pronounced changes in vegetation greenness occurred.

4.3. Mean NDVI results

The mean NDVI results indicate that most of the study area falls within the sparse vegetation class, which accounts for 69.20% of the analysed area. Very sparse vegetation covers a further 24.49%. Together, these classes represent 93.69% of the basin, indicating predominantly low to intermediate mean vegetation greenness during March–October 2025 (**Fig. 5**).

Moderate vegetation cover (0.4–0.6) accounts for 6.02% of the study area, while dense vegetation (0.6–1.0) occupies a negligible proportion, less than 0.01%. Non-vegetated areas (−1–0) represent 0.29%. These categories describe the distribution of mean NDVI values and should not be interpreted as direct measurements of vegetation density or land-cover composition.

The predominance of the sparse and very sparse vegetation classes may reflect both limited vegetation cover and seasonal variation in agricultural fields and grasslands. Averaging NDVI across the growing season combines periods of active growth with periods of reduced vegetation activity or exposed soil. Consequently, a low mean NDVI does not necessarily indicate persistent sparse vegetation or land degradation, while a higher mean NDVI does not establish that vegetation activity remained stable throughout the season.

Overall, mean NDVI summarises spatial differences in vegetation greenness across the basin during the analysed period. Its interpretation alongside monthly NDVI and ΔNDVI helps distinguish seasonal patterns that are not apparent from the growing-season mean alone.

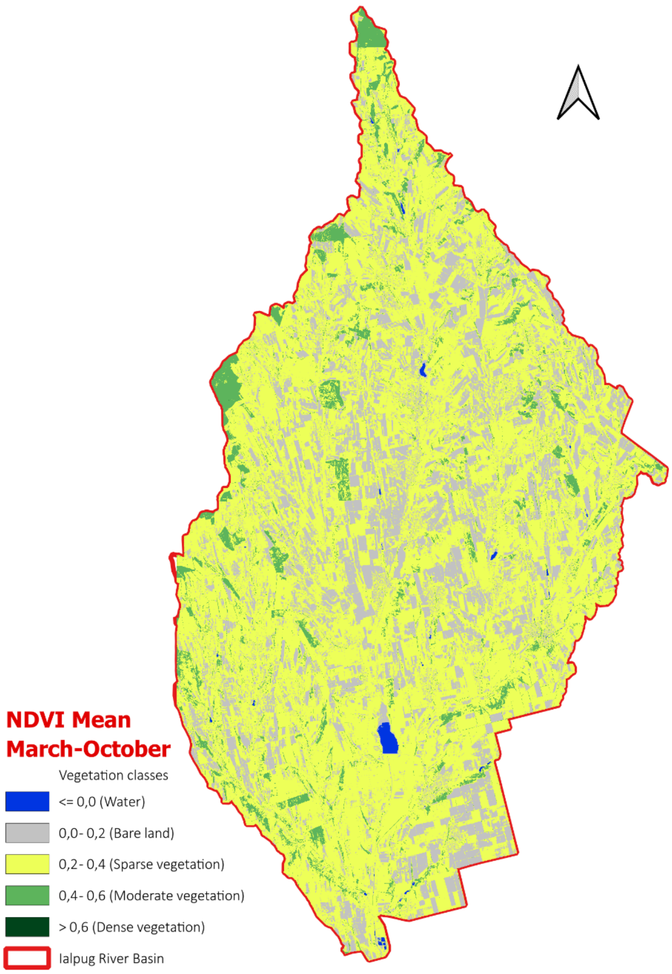

Fig. 5. Mean NDVI for the period March–October 2025.

5. DISCUSSION

The seasonal NDVI pattern in the analysed part of the Ialpug River Basin is consistent with vegetation development in an agricultural landscape, where crop phenology and environmental conditions may produce overlapping changes in greenness. The contrasting increases and decreases observed between May and June suggest that vegetation development was spatially asynchronous before the widespread decline between June and July. Meroni et al. (2021) demonstrated that Sentinel-2 NDVI time series can describe crop-specific seasonal development across Europe, supporting the relevance of crop calendars when interpreting these patterns. However, the present analysis did not distinguish individual crop types, so their respective contributions to the observed changes remain unresolved.

The summer NDVI decline coincided with hot and dry conditions documented in southern Moldova. The State Hydrometeorological Service reported mean air temperatures 1.5–2.5°C above the climatic norm during June–August 2025, precipitation totals of approximately 45–75 mm and SPEI values between −1.1 and −1.9, indicating moderate to severe drought (Serviciul Hidrometeorologic de Stat, 2025). These observations make water stress a plausible contributor to the decline in vegetation greenness. Nevertheless, the regional climatic information was used as contextual evidence and was not statistically related to the NDVI observations. The respective effects of drought, crop maturation, harvesting and natural senescence therefore cannot be separated by the present analysis.

The predominance of the sparse vegetation and very sparse vegetation classes in the mean NDVI raster indicates that average greenness was relatively low across most of the study area. However, similar mean values can arise from different seasonal trajectories, including consistently low greenness or a pronounced growing period followed by harvesting or senescence. Conversely, a higher mean does not demonstrate uninterrupted vegetation activity. The near-absence of the dense vegetation class in the mean raster therefore does not establish the absence of dense vegetation at individual observation dates. Mean NDVI is most informative when interpreted together with the monthly NDVI and ΔNDVI maps, which retain information about the timing and direction of change.

The environmental interpretation of these patterns is constrained by the coverage of a single growing season and the absence of independent land-cover information and field validation. Low or declining NDVI may correspond to sparse vegetation, crop maturation, harvested fields, exposed soil or vegetation stress, which have different implications for land management. The observations therefore identify seasonal differences in greenness but do not establish persistent land degradation, aridization or ecological resilience. Such interpretations require evidence that distinguishes expected seasonal variation from sustained changes in vegetation condition.

The classification also introduces uncertainty. Soil background can influence NDVI where vegetation cover is limited, while the adopted thresholds group continuous spectral variation into broad categories. These categories were not calibrated against field measurements or individual land-cover types and should therefore be treated as descriptive NDVI classes rather than verified measures of vegetation density, health or degradation. Likewise, the ΔNDVI thresholds distinguish changes by their numerical magnitude; they do not represent statistical significance or independently validated ecological responses.

Temporal sampling further limits the interpretation. Each monthly map represents one selected monthly mosaic rather than a monthly composite so short-lived growth or stress events may be missed. In addition, the April and June mosaics combine northern and southern tiles acquired two days apart, meaning that each mosaic is not a strictly simultaneous observation of the entire study area. The intervals between successive acquisitions also vary, so ΔNDVI describes change between the selected dates rather than a standardized rate of change. The mean raster consequently summarizes the eight selected monthly mosaics rather than a continuously observed growing-season average.

Further research should combine a denser, multi-year Sentinel-2 time series with land-cover information, crop calendars and meteorological observations matched to the study area. Comparison with precipitation, temperature, soil moisture and drought indices would allow vegetation responses to be evaluated against climatic variability, while field observations would help validate the interpretation of the NDVI classes. This would provide a basis for distinguishing recurrent agricultural cycles from unusual vegetation decline and for assessing whether low greenness persists across years. The present maps can guide this work by identifying locations with contrasting seasonal trajectories for targeted investigation.

6. CONCLUSIONS

The combined analysis of monthly NDVI, ΔNDVI and mean NDVI characterized seasonal vegetation greenness in the analysed Moldovan part of the Ialpug River Basin during March–October 2025. Their joint interpretation distinguished vegetation condition at selected observation dates, changes between observations and average greenness across the study period, providing a basis for screening seasonal vegetation dynamics.

The seasonal pattern comprised spring greening, spatially contrasting changes in early summer and widespread decline between June and July, when 54.18% of the study area recorded an NDVI decrease exceeding 0.1. Moderate vegetation cover occupied its largest share in April, while dense vegetation reached its maximum extent in June. Low NDVI classes subsequently predominated, with very sparse vegetation reaching its greatest extent in September. October showed limited greening, without a return to the spring distribution of vegetation classes.

The mean NDVI classification placed 69.20% of the study area in the sparse vegetation class and 24.49% in the very sparse vegetation class, together accounting for 93.69%. These proportions indicate predominantly low average greenness across the selected observations. They do not establish that vegetation remained sparse throughout the season, because the same mean value can reflect different combinations of growth and decline.

The resulting maps can support preliminary monitoring by identifying areas with pronounced seasonal decline or low average greenness for further investigation. Although the summer decline coincided with documented regional drought conditions, the analysis does not isolate its causes or demonstrate persistent land degradation. Multi-year observations and independent climatic, land-cover and field evidence are needed before these patterns can support conclusions about long-term environmental change.

REFERENCES

Burduja, D. and Bacal, P. (2023) Regional aspects of water use and management in the Republic of Moldova. *Central European Journal of Geography and Sustainable Development*, 5(2), pp. 62–84. doi: 10.47246/CEJGSD.2023.5.2.4.

Chiriac, I. and Sirodoev, G. (2025) The Ialpug River Basin: Location on the map of administrative-territorial units. *Research – Innovation – Innovative Entrepreneurship: International Scientific Congress*, 3rd edn, 7–8 June 2025, vol. II, pp. 168–176. doi: 10.46727/c.v2.07-08-06-2025.p168-176.

Copernicus Data Space Ecosystem (n.d.) *Sentinel-2*. Available at: https://dataspace.copernicus.eu/data-collections/copernicus-sentinel-missions/sentinel-2 (Accessed: 5 September 2026).

Eisfelder, C., Asam, S., Hirner, A., Reiners, P., Holzwarth, S., Bachmann, M., Gessner, U., Dietz, A., Huth, J., Bachofer, F. and Kuenzer, C. (2023) Seasonal vegetation trends for Europe over 30 years from a novel Normalised Difference Vegetation Index (NDVI) time series – the TIMELINE NDVI product. *Remote Sensing*, 15(14), 3616. doi: 10.3390/rs15143616.

Gabriele, M., Brumana, R., Previtali, M. and Cazzani, A. (2023) A combined GIS and remote sensing approach for monitoring climate change-related land degradation to support landscape preservation and planning tools: The Basilicata case study. *Applied Geomatics*, 15, pp. 497–532. doi: 10.1007/s12518-022-00437-z.

Govedar, Z. and Anikić, N. (2024) Vegetation indices monitoring by using Copernicus data in the old-growth forests of the Republic of Srpska/Bosnia and Herzegovina. *Frontiers in Forests and Global Change*, 7, 1354769. doi: 10.3389/ffgc.2024.1354769.

Guvernul Republicii Moldova (2023) *Hotărârea Guvernului nr. 624 din 30 august 2023 cu privire la aprobarea Programului național de adaptare la schimbările climatice până în anul 2030*. Chișinău: Guvernul Republicii Moldova. Available at: https://www.legis.md/cautare/getResults?doc_id=140163&lang=ro (Accessed: 28 June 2026).

Huang, S., Tang, L., Hupy, J.P., Wang, Y. and Shao, G. (2021) A commentary review on the use of normalized difference vegetation index (NDVI) in the era of popular remote sensing. *Journal of Forestry Research*, 32(1), pp. 1–6. doi: 10.1007/s11676-020-01155-1.

Jeleapov, A. (2024) Evaluarea dinamicii curgerii de apă a râului Ialpug [Evaluation of flow dynamics of the Ialpug River]. In: *Mediul și dezvoltarea durabilă: Conferință științifică națională cu participare internațională*, 6th edn, 17–18 May 2024. Chișinău: CEP UPSC, pp. 104–114. doi: 10.46727/cg.17-18-05-2024.p104-114.

Karlsen, S.R., Stendardi, L., Tømmervik, H., Nilsen, L., Arntzen, I. and Cooper, E.J. (2021) Time series of cloud-free Sentinel-2 NDVI data used in mapping the onset of growth of central Spitsbergen, Svalbard. *Remote Sensing*, 13(15), 3031. doi: 10.3390/rs13153031.

Meroni, M., d'Andrimont, R., Vrieling, A., Fasbender, D., Lemoine, G., Rembold, F., Seguini, L. and Verhegghen, A. (2021) Comparing land surface phenology of major European crops as derived from SAR and multispectral data of Sentinel-1 and -2. *Remote Sensing of Environment*, 253, 112232. doi: 10.1016/j.rse.2020.112232.

Phiri, D., Simwanda, M., Salekin, S., Nyirenda, V.R., Murayama, Y. and Ranagalage, M. (2020) Sentinel-2 data for land cover/use mapping: A review. *Remote Sensing*, 12(14), 2291. doi: 10.3390/rs12142291.

Rossi, V., Krtalić, A. and Buzjak, N. (2025) Land cover mapping in mountainous Croatia using Sentinel-2A satellite imagery. *Environmental Earth Sciences*, 84, 499. doi: 10.1007/s12665-025-12510-y.

Serban, C. and Maftei, C. (2025) Remote sensing evaluation of drought effects on crop yields across Dobrogea, Romania, using Vegetation Health Index (VHI). *Agriculture*, 15(7), 668. doi: 10.3390/agriculture15070668.

Serviciul Hidrometeorologic de Stat (2022) *Evaluarea resurselor climatice ale precipitațiilor atmosferice pe teritoriul Republicii Moldova prin prisma schimbărilor climatice*. Available at: https://www.meteo.md/images/uploads/gis/Evaluarea_precipitatiilor_2022.pdf (Accessed: 27 June 2026).

Serviciul Hidrometeorologic de Stat (2025) *Caracterizarea condițiilor meteorologice și agrometeorologice din vara anului 2025*. Available at: https://www.meteo.md/images/uploads/clima/2025/vara2025_ro.pdf (Accessed: 27 June 2026).

Smith, T. and Boers, N. (2023) Reliability of vegetation resilience estimates depends on biomass density. *Nature Ecology & Evolution*, 7, pp. 1799–1808. doi: 10.1038/s41559-023-02194-7.

Tian, F., Cai, Z., Jin, H., Hufkens, K., Scheifinger, H., Tagesson, T., Smets, B., Van Hoolst, R., Bonte, K., Ivits, E., Tong, X., Ardö, J. and Eklundh, L. (2021) Calibrating vegetation phenology from Sentinel-2 using eddy covariance, PhenoCam, and PEP725 networks across Europe. *Remote Sensing of Environment*, 260, 112456. doi: 10.1016/j.rse.2021.112456.

Tucker, C.J. (1979) Red and photographic infrared linear combinations for monitoring vegetation. *Remote Sensing of Environment*, 8(2), pp. 127–150. doi: 10.1016/0034-4257(79)90013-0.

Varghese, D., Radulović, M., Stojković, S. and Crnojević, V. (2021) Reviewing the potential of Sentinel-2 in assessing the drought. *Remote Sensing*, 13(17), 3355. doi: 10.3390/rs13173355.

Vicente-Serrano, S.M., Juez, C., Potopová, V., Boincean, B., Murphy, C., Domínguez-Castro, F., Eklundh, L., Peña-Angulo, D., Noguera, I., Jin, H., Conradt, T., García-Herrera, R., Garrido-Pérez, J.M., Barriopedro, D., Gutiérrez, J.M., Iturbide, M., Lorenzo-Lacruz, J. and El Kenawy, A. (2024) Drought risk in Moldova under global warming and possible crop adaptation strategies. *Annals of the New York Academy of Sciences*, 1538(1), pp. 144–161. doi: 10.1111/nyas.15201.

Von Keyserlingk, J., de Hoop, M., Mayor, A.G., Dekker, S.C., Rietkerk, M. and Foerster, S. (2021) Resilience of vegetation to drought: Studying the effect of grazing in a Mediterranean rangeland using satellite time series. *Remote Sensing of Environment*, 255, 112270. doi: 10.1016/j.rse.2020.112270.